Triple-junction amorphous silicon alloy solar cell with 14.6% initial and 13.0% stable conversion efficiencies

J. Yang, A. Banerjee, and S. Guha
United Solar Systems Corporation, Troy, Michigan 48084

(Received 28 January 1997; accepted for publication 2 April 1997)

We have achieved 14.6% initial and 13.0% stable conversion efficiencies using an amorphous silicon-based alloy in a spectrum-splitting, triple-junction structure. These efficiencies have been confirmed independently by the National Renewable Energy Laboratory. Key factors leading to this major advance include improvements made in the low band-gap amorphous silicon–germanium alloy cell, the *pn* tunnel junction between the component cells, and the top conducting oxide. © *1997 American Institute of Physics.* [S0003-6951(97)00222-2]

Amorphous silicon (*a*-Si) alloy photovoltaic technology has received a great deal of attention due mainly to its low material cost and ease of manufacturing.[1] One major challenge, however, is to improve the stable module efficiency to 15%.[2] We report in this letter that significant progress has been made in (1) the low band-gap amorphous silicon–germanium (*a*-SiGe) alloy cell that resulted in enhanced red response and provided desirable current mismatching, (2) the *pn* tunnel junction between the component cells by incorporating microcrystalline *p* and *n* layers in a multilayered structure that resulted in reduced optical and electrical losses, and (3) the top conducting oxide that resulted in reduced absorption and enhanced blue response. Incorporating these advances in a spectrum-splitting, triple-junction structure, a 14.6% initial active-area conversion efficiency has been achieved and independently measured by the National Renewable Energy Laboratory (NREL) to be 14.5%. The stabilized efficiency after 1000 hours of one-sun light soaking of this device is 13.0%. Both initial and stable efficiencies represent the highest values reported to date for *a*-Si alloy solar cells.

Figure 1 shows a schematic diagram of a triple-junction structure. The top intrinsic (*i*) layer uses a wide band-gap *a*-Si alloy for absorbing the blue photons, while the middle and bottom *i* layers incorporate intermediate and low band-gap *a*-SiGe alloys with different silicon-to-germanium ratios for absorbing the green and red photons, respectively. A textured silver/zinc-oxide back reflector[3] is used to facilitate light trapping. The red photons that reach the back surface are scattered back at an oblique angle for additional optical path and absorption in the *i* layers. The top contact uses evaporated indium–tin–oxide (ITO), which also serves as an antireflection coating. Finally, a metal grid is deposited on top of the ITO for collecting current.

All three *i* layers use heavy hydrogen dilution during film growth to obtain better cell performance;[4] in addition, the *a*-SiGe alloy *i* layers employ band-gap profiling to obtain better carrier collection.[5] Microcrystalline *p* layers[6] with high conductivity and low optical absorption are used as the window layer, as well as in the tunnel junctions.

Using the above approach, along with an appropriate current mismatching cell design, we have recently reported 13.2% initial and 11.8% stable cell efficiencies.[7] Figure 2 shows the initial quantum efficiency (*Q*) data, exhibiting the blue, green, and red spectrum splitting of the triple structure. It is noted that the total photocurrent generated in the triple stack is $\sim 25\ \mathrm{mA/cm^2}$. A careful analysis leads us to believe that it is possible to enhance the photocurrent generation and collection in the three wavelength regimes: (1) the response in the long-wavelength ($\lambda > 800$ nm) region, (2) the response associated with the absorption of the tunnel junction between the top and the middle cells in the $\lambda \sim 500-600$ nm region, and (3) the response in the short-wavelength ($\lambda < 450$ nm) region.

One way to enhance the long-wavelength response is to increase the germanium content in the bottom cell. This, however, often results in a poorer material quality and deteriorates the solar cell performance. By optimizing hydrogen dilution during film growth and incorporating proper band-gap profiling, we have been successful in improving the performance of the bottom cell and have obtained a 10.37% efficiency under AM 1.5 illumination. The corresponding quantum efficiency data show a 45% collection at 850 nm, a significant improvement over our previous value of 35%.

There are two tunnel junctions in the triple structure (see Fig. 1); one is p_2n_3 between the top and the middle cells, and

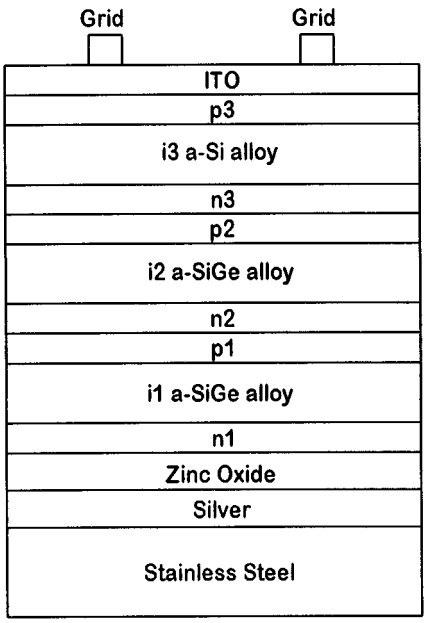

FIG. 1. Schematic diagram of a triple-junction cell structure.

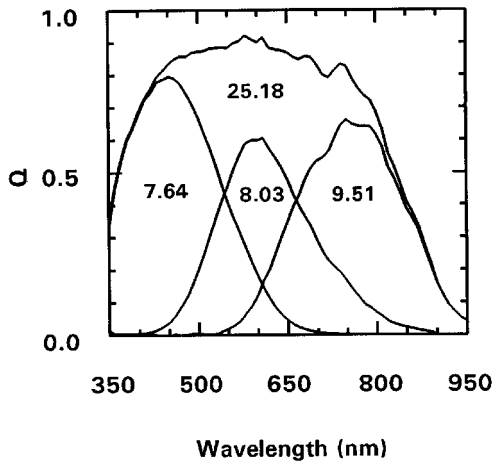

FIG. 2. Initial quantum efficiency of the previous triple cell.

the other is p_1n_2 between the middle and the bottom cells. Any reduction in their optical absorption or electrical resistance, for example, by using microcrystalline doped layers, should give rise to a better cell performance. In our earlier triple-junction cells, we used microcrystalline p layers but amorphous n layers. We have carried out a study to evaluate the benefit of using both microcrystalline p and n layers in the tunnel junctions. Since the p_2n_3 top tunnel junction is closer to where light enters the device than the p_1n_2 bottom tunnel junction, any improvement in the p_2n_3 top tunnel junction is expected to result in a larger improvement in the cell performance.

To evaluate the top tunnel junction, we studied a pair of a-Si/a-Si double-junction cells made under substantially the same deposition conditions. The only difference between the two devices is that one uses an amorphous n layer, while the other uses a microcrystalline n layer in the tunnel junction. Even though the use of the microcrystalline n layer allowed more light to go to the bottom cell, as evidenced by its higher short-circuit current density, we found, to our surprise, that the V_{oc} value for the tandem cell having a microcrystalline n layer is much lower ($V_{oc}=1.657$ V) than the corresponding cell with an amorphous n layer ($V_{oc}=1.804$ V) in the tunnel junction. We attribute the lowering of V_{oc} to the following two reasons: First, since microcrystalline material is expected to have a lower band-gap than its amorphous counterpart, there may be a band-edge discontinuity[8] between the amorphous i and microcrystalline n layers resulting in the lowering of V_{oc}. Second, since deposition conditions for microcrystalline materials generally require high rf power and high hydrogen dilution,[6] these conditions may cause the intermixing of the dopants in the thin doped layers, thus, the lowering of V_{oc}.

We have developed a thin buffer layer that can be inserted between the microcrystalline p and n layers and also between the microcrystalline n and the adjacent amorphous i layers to alleviate the problem. We compared two tandem cells, one with a conventional amorphous n layer and the other with the new multilayered structure in the tunnel junction; the results are listed in Table I. Incorporation of the new tunnel-junction structure gives rise to improved cell characteristics, as evidenced by the higher total current and lower series resistance.

The top conducting oxide serves as the top contact as well as an antireflecting coating. If one can reduce the absorption in ITO without lowering its conductivity, one should gain in photocurrent. This will benefit the entire triple stack with the top cell receiving the most advantage. We have reoptimized the ITO evaporation conditions by adjusting the oxygen partial pressure and obtained a more transparent film. A top cell deposited onto a stainless-steel substrate with the improved ITO layer shows $J_{sc}=8.68$ mA/cm^2, $V_{oc}=1.011$ V, and $FF=0.782$; the J_{sc} value is ~ 0.5 mA/cm^2 higher than that obtained from a similar cell with the previous ITO. The higher current is obtained without increasing the i layer thickness, which is certainly desirable from the stability point of view. The J_{sc} value of ~ 8.5 mA/cm^2 is also suitable for the top cell of a triple structure with the enhanced red response in the bottom cell.

Incorporating the above improvements, several triple cells with initial efficiencies exceeding 14% were obtained. The highest efficiency achieved is 14.6%, and the $J-V$ characteristics are summarized in Table II. This represents a major improvement over our previous record of 13.2%. Compared to our earlier best triple cell, one notices that J_{sc} is increased from 7.64 to 8.57 mA/cm^2, while V_{oc} and FF values remain similar. Quantum efficiency data plotted in Fig. 3 reveal that the total photocurrent from the triple stack is 26.88 mA/cm^2, significantly higher than our earlier value of 25.18 mA/cm^2 (see Fig. 2). Comparing Figs. 2 and 3, one can readily see that (1) the quantum efficiency for $\lambda > 800$ nm is increased due to the enhancement of the red response, (2) the quantum efficiency for the $\lambda \sim 500-600$ nm region is improved due to the incorporation of the new pn tunnel junction, and (3) the overall quantum efficiency is increased, especially in the $\lambda < 450$ nm region, due to the improvement in ITO. We, indeed, benefit from the three advances discussed above.

A few high efficiency devices were sent to the NREL for triple-source measurement. Device L8605 gives the best characteristics, as summarized in Table II. It should be pointed out that the J_{sc} value at United Solar is based on the

TABLE I. Characteristics of a-Si/a-Si tandem cells with different tunnel-junction structures.

Tunnel-junction structure	J_{sc} (mA/cm^2)	V_{oc} (V)	FF	η (%)	Q_{top} (mA/cm^2)	Q_{btm} (mA/cm^2)	Q_{total} (mA/cm^2)	R_s (Ω cm^2)
Microcrystalline p amorphous n	7.80	1.901	0.752	11.15	7.97	7.8	15.77	15.0
Microcrystalline p multilayered n	8.06	1.919	0.766	11.85	8.06	8.28	16.34	14.3

TABLE II. Initial and stable triple-cell efficiency (area of ~ 0.25 cm^2) as measured at United Solar and NREL.

Device L8605	V_{oc} (V)	I_{sc} (mA)	FF (%)	J_{sc} (total area) (mA/cm^2)	η (total area) (%)	J_{sc} (active area) (mA/cm^2)	η (active area) (%)	Measurement laboratory
Initial	2.357		72.3			8.57	14.6	United Solar
Initial	2.357	2.104	74.39	7.721	13.5	8.28	14.5	NREL
Stable	2.294		68.4			8.27	13.0	United Solar
Stable	2.297	2.061	69.7	7.563	12.1	8.11	13.0	NREL

quantum efficiency measurement. The NREL measures the total area efficiency only; the active-area current density is obtained by first subtracting the grid coverage from the total area and then calculating its active-area current density. It is readily seen that the active-area efficiency values agree well between the two laboratories.

The devices were then subjected to indoor light soaking under one-sun, 50 °C, and open-circuit conditions. After ~ 300 h of exposure, the cell performance was substantially stabilized. The $J-V$ characteristics after light soaking for 1000 h for device L8605 are also listed in Table II, showing a stabilized efficiency of 13.0%. This is the highest stable

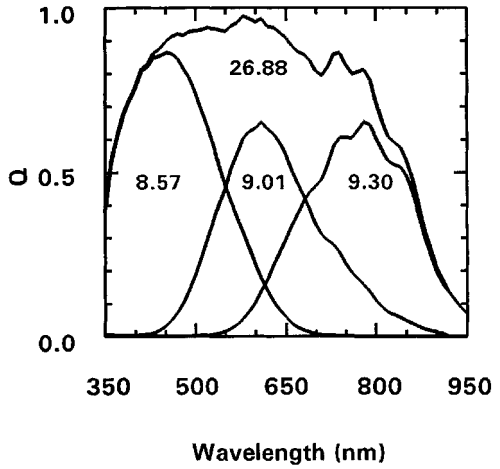

FIG. 3. Initial quantum efficiency of the improved triple cell.

conversion efficiency for a-Si alloy solar cells reported to date. The cell efficiency has also been confirmed by the NREL (Table II). Further improvement in the understanding of plasma chemistry, film growth, and the light-induced degradation mechanism should help in further enhancing the cell efficiency.

The authors thank E. Chen, G. Hammond, M. Hopson, N. Jackett, H. Laarman, J. Noch, and T. Palmer for their assistance in the sample preparation and measurements, S. R. Ovshinsky, X. Xu, S. Sugiyama, T. Glatfelter, and R. Crandall for stimulating discussions, and V. Trudeau for help in manuscript preparation. The work was supported in part by NREL under Subcontract Nos. ZAN-4-13318-02 and ZAF-5-14142-01.

[1] S. Guha, J. Yang, A. Banerjee, T. Glatfelter, K. Hoffman, S. R. Ovshinsky, M. Izu, H. C. Ovshinsky, and X. Deng, Mater. Res. Soc. Symp. Proc. **645**, 1994.
[2] W. Luft, H. M. Branz, V. L. Dalal, S. S. Hegedus, and E. A. Schiff, AIP Conf. Proc. **306**, 31 (1993).
[3] R. Ross, R. Mohr, J. Fournier, and J. Yang, Proc. 19th IEEE PVSC, 327 (1987).
[4] J. Yang, A. Banerjee, T. Glatfelter, K. Hoffman, X. Xu, and S. Guha, Proceedings of the First World Conference on Photovoltaic Energy Conversion, 380 (1994).
[5] S. Guha, J. Yang, A. Pawlikiewicz, T. Glatfelter, R. Ross, and S. R. Ovshinsky, Appl. Phys. Lett. **54**, 2330 (1989).
[6] S. Guha, J. Yang, P. Nath, and M. Hack, Appl. Phys. Lett. **49**, 218 (1986).
[7] J. Yang, X. Xu, A. Banerjee, and S. Guha, Proc. 25th IEEE PVSC, 1041 (1996).
[8] X. Xu, J. Yang, A. Banerjee, S. Guha, K. Vasanth, and S. Wagner, Appl. Phys. Lett. **67**, 2323 (1995).